

# High Performance Multilayered High Temperature Cofired Ceramic for Wide Band Packaging

Christophe A. Tavernier<sup>1</sup>, Frédéric Valentin<sup>2</sup>, Mohammed Mazouz<sup>3</sup>, Roberto Vigo<sup>1</sup>,  
Wladimir Muffato<sup>1</sup>, Philippe Maeder<sup>1</sup>, Marc Havasi<sup>1</sup>

<sup>1</sup>EGIDE, egide@egide.fr, Trappes, 78190, France, <sup>2</sup>Universite de Limoges, DESS microndes, Limoges France, <sup>3</sup>DalightCom, Les Loges en Josas, France

**Abstract** — Opto-electronic and wireless packages have to meet stringent technical performance and cost. Traditionally glass sealed metal machined packages respond to the demand. In 2003, with ever growing complexity, new technology now offers advantageous solutions. While keeping high hermiticity, low mechanical tolerance and electromagnetic compatibility, multilayered ceramic offers a superior flexibility at a lower cost. The present article provides insight on High Temperature Cofired Ceramic (HTCC) achievable electrical performance in the DC to 40 GHz range based on FEM modeling with Ansoft HFSS. We compare model and experimental results for ring and cavity resonators with quality factor up to 180. Based on the model we then derive wide band asymmetrical stripline and vertical interconnect.

**Index terms** — HTCC, wide band ceramic package, HFSS modeling, ring resonator, cavity resonator, EBG structure, asymmetric stripline, vertical interconnect.

## I. INTRODUCTION

EGIDE's expertise in glass sealed and ceramic packages yield protective package for the OC48 up to OC768 chips used in the long haul and metropolitan fiber optics networks. Packages provide mechanical strength and tight tolerances for optical alignment, high thermal dissipation, and electromagnetic compatibility, while keeping wide band signal electrical and optical integrity. Quality assurance standards such as MIL-STD-883 and Bellcore Telcordia for opto electronics are used, along with more stringent requirements for military and space applications where EGIDE is also a package manufacturer. Incorporation of the performance requirements can be as much as one-third of the complete module price.

To achieve performance and reduce cost, packaging technology development has to respond to optical, thermal, mechanical and electrical constraints. HTCC has the following properties: it is 92% pure Alumina (cofired at 1600°C); offers high mechanical hardness and strength (Young modulus  $3.10^6$  kg/cm<sup>2</sup>); provides acceptable heat dissipation (22 W/m.°C – improved with thermal vias [1]); has TCE compatibility with Kovar, BK7 glass and sapphire; and is chemical stable with low dielectric loss ( $\tan \delta < 8.10^{-4}$  at 10 GHz [5]). Metal interconnect is made

by screen printing thick film Tungsten line with Nickel and Gold finish. The hermetic fabrication (pressure  $< 10^{-8}$  atm.) ensures oxygen free atmosphere in the package for many years. Recently multilayered ceramic layers moved towards thinner layer thickness (below 100  $\mu\text{m}$ ) which permits small via diameter (below 100  $\mu\text{m}$ ). In parallel, metal line conductivity improved by using copper alloy so that electrical attenuation is reduced [2].

For electrical performance estimation, resonators and transmission lines give accurate results leading to the development of accurate FEM based package models, which are valid for wide band applications.

## II. RING AND CAVITY RESONATORS

Resonators are classical circuits that give a good estimate of the substrate permittivity [3], [4], [5]. With a narrow gap between line and ring, well defined resonance with high return loss is obtained (70  $\mu\text{m}$  in the current design). Equation (1) defines the resonance and its quality factor with  $l$  being the ring perimeter and  $n$  an integer.

$$f_{\text{res}} = \frac{n.c}{2.l.\sqrt{\epsilon_{\text{eff}}}}; Q_u = \frac{f_{\text{res}}}{\Delta f_{3\text{dB}}} \cdot 10^{-|S_{21}(\text{dB})|/20} \quad (1)$$

For on-wafer testing, a CPW-to-microstrip transition is used to connect to the network analyzer. The quality of the transition is less than 10 dB return loss up to 28 GHz with less than 0.1 dB/mm attenuation up to 20 GHz.

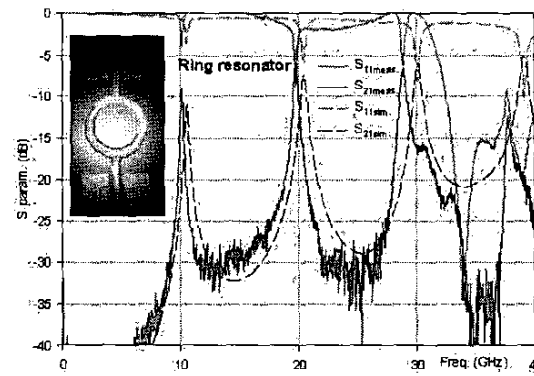


Fig. 1. Simulated vs. measured performance of ring resonator.

As seen on Fig. 1, measured and modeled resonator performance have good correlation up to 30 GHz. The frequency shift describes the increasing ceramic permittivity which is considered constant in the model. Reproducibility is tested among 10 random samples. It resulted in less than 25 MHz error on the resonance which is less than the measurement error range.

The unloaded quality factor reaches 160 at 10 GHz ( $S_{21} = -9.1$  dB,  $\Delta f = 180$  MHz, with  $f_{res} = 10.1$  GHz). This value is higher than the one in the model where gold surface finish is not included.

Compared to the ring resonator, the cavity resonator design [6] constrains the field entirely in the ceramic. The resulting sensitivity yields an accurate estimation of the dielectric loss tangent. In addition, the evaluation of the grounding via quality is made possible when implementing an EBG-type structure. Such design is described in [7], here with a circular configuration for performance improvement [8]. When radius  $r$  is larger than half the cavity height,  $h$ , the frequency of the  $TE_{10}$  fundamental mode resonance can be described by (2):

$$f_{010}^{TM} = \frac{2.405 \times c}{2\pi r \sqrt{\epsilon_{eff}}}; Q = \frac{1.2 \times 377 \times \sqrt{\sigma}}{(1 + h/2r) \cdot \sqrt{\pi \cdot f \cdot \mu_0 \cdot \epsilon_{eff}}} \quad (2)$$

Via posts can be used to replace the metallic wall, with a distribution of 2 rows of equally spaced vias. Using equation (2), 6 designs are derived with resonant frequency at 15, 20, 25, 28, 34, and 38 GHz. The corresponding cavity radii vary from 2.4 to 1 mm. The access line to cavity consists of the previous CPW-to-microstrip line transition. At the end of it, a short circuiting via next to a slot in the ground plane realizes a magnetic coupling in the underneath cavity.

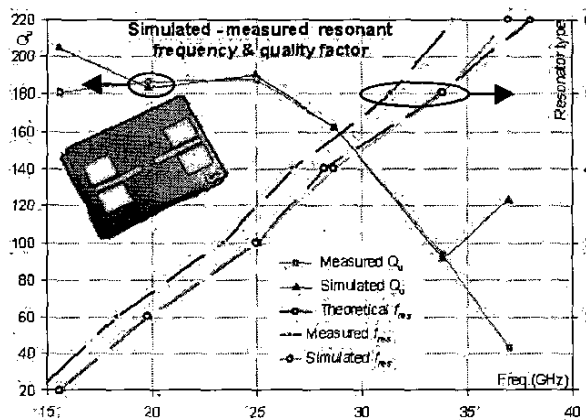


Fig. 2. Simulated vs. measured performance of cavity resonator: resonant frequency and unloaded quality factor.

Measured and modeled performance are compared in Fig. 2 and Fig. 5 for the 6 configurations. Good correlation is found up to 34 GHz. The constant permittivity used in the model again explains the frequency shift (Fig. 2). Good reproducibility is obtained in the measurement.

Using (1), the quality factor ranges above 170 up to 25 GHz (Fig. 2). It decays linearly between 25 and 34 GHz. Because of the metal conductivity limitation [7], loss increases with frequency and the quality factor simultaneously drops. This can be explained by a higher surface current density in the cavity when the design dimensions become smaller. In other words high frequency designs have smaller size and therefore higher surface current density at the resonance. This explains the increment of metal loss in the conductive cavity wall and ground planes.

Beyond 34 GHz, model and experimental results show significant divergence. Although, the roughness [5] of the metal conductors is not included in the model, roughness accounts for a conductivity drop with frequency (see [2] relating to Tanaka *et al.*). It is expressed in formula (3):

$$\sigma_{rough} = \frac{\sigma}{(1 + \exp(-\frac{1}{2 \cdot R_a \cdot \sqrt{\pi \cdot f \cdot \mu_0 \cdot \sigma}})^{1.6})^2} \quad (3)$$

where  $R_a$  is the average surface roughness of the metal lines. With improvement to the process, this value can be reduced and the transmission improved [5].

### III. LINES & VERTICAL INTERCONNECT - MODEL

The high quality of the previous model makes it suitable to design wide band transmission structures. Using it, we derived horizontal  $50\ \Omega$  striplines and vertical interconnect [9] - (Fig. 3) and (Fig. 4).

To test isolation, several lines are fabricated on a single substrate. Asymmetrical stripline is implemented for metal loss reduction. Two GCPW lines on each side of the stripline provide access to the probe system. Grounding is achieved by periodical vias distributed in the first and last ceramic layer. Open vias on each side of the stripline section improve grounding.

As shown on Fig. 3, measurement and model response compare well together. Due to surface roughness and extension of ground plane, the insertion loss is high in the 30 to 40 GHz range. Nevertheless the design shows no cutoff up to 36 GHz, as predicted by the model. Design improvement consisted of reducing the ceramic extension behind the access line that generates coupling. Increased bandwidth of the 8.7 mm long line can be obtained by further reducing the size of the cavity made by the

grounding vias. Overall performance is summarized in the Table 1:

Freq. (GHz)	10	20	30	36
$S_{11}$ (dB)	< -20	< -20	< -18	< -15
$S_{21}$ (dB)	-0.4	-0.8	-1	-1.4

Table 1. Measured performance of asymmetric stripline

Measurement results shows a high return loss above 29 GHz which is not predicted by the model. Knowing that the model is identical to the one used in the previous section, this suggests a measurement issue which will be addressed in the near future.

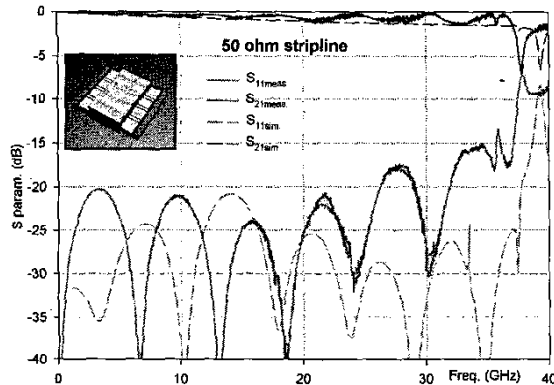


Fig. 3. Simulated vs. measured performance of stripline.

Another type of transmission study is proposed with vertical interconnections [9]. It allows microwave signal propagation though the ceramic layers. The signal is carried through vias between two CPW transmission lines at two different heights. In such design, alignment and grounding are critical for proper matching and low attenuation. The inductance of the design is reduced by using small via size.

The performance is estimated on Fig. 4 using the previous model characteristics. Such a vertical interconnect can be utilized to report the package on the PC board with leadframes or Ball Grid Array. The model of Fig. 4 estimates the later one.

In HFSS modeling, conservative estimates for the conductor lines were used. We applied a conductivity value of  $5.10^6$  S/m to the metallized surfaces and vias. Lines are modeled as 2D structures and a radiating boundary condition box surrounds the design and wave ports in order to model free space [9]. In the HFSS material setup, HTCC layers are Alumina with permittivity 9.2 and  $7.7 \times 10^{-4}$  loss tangent at 10 GHz.

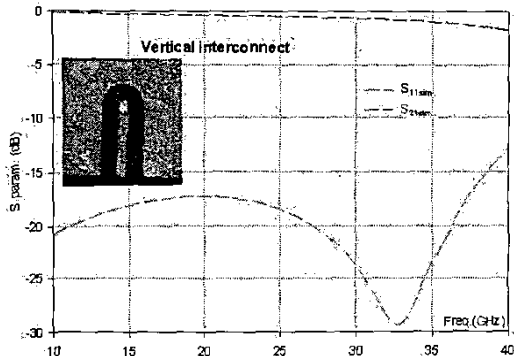


Fig. 4. Vertical interconnect performance based on HFSS modeling.

## V. CONCLUSION

In this article, we gave an overview of performance achieved using model and experimental work on multilayer High Temperature Cofired Ceramic, an efficient and cost effective material for opto-electronics and wireless packaging. We designed and tested ring and cavity resonators. After agreement was found between experiment and the FEM modeling technique, we then studied transmission line and vertical interconnect in the 0 to 40 GHz range.

The quality factor of resonators is greater than 170 up to 25 GHz. It then linearly decays due to metal conductivity, reaching 100 at 34 GHz. Conductor roughness and coupling further reduce the performance which diverges from the model prediction.

Transmission lines showed less than 18 dB return loss in the 0 to 30 GHz range and less than 15 dB up to the cutoff at 36 GHz. Low attenuation is reached, 0.046 dB/mm at 10 GHz and 0.092 dB/mm at 20 GHz. Performance compares well with existing work using connectorized solutions [10]. Based on the model, vertical interconnections using vias were derived as well. The model predicts better than 18 dB return loss in the 0 – 38 GHz range.

Future work will focus on reducing the loss at frequency above 34 GHz. In addition layout options to reduce coupling and process improvements to reduce surface roughness issues will be addressed, larger bandwidth transmission lines will be studied as well. Currently measurement of the vertical interconnect is underway.

## ACKNOWLEDGEMENT

The authors wish to acknowledge the work of the EGIDE's design center and manufacturing plant in Bollène France.

## REFERENCES

- [1] P. J. Gielisse, H. Niculescu, J. Tremblay, S. Achmatowicz, M. Jakobowski, E. Zwierkowska, L. Golonka, "Wide Bandgap Materials in Thermal Management of Electronic Structure", *IEEE*, pp. 36-37, 2001.
- [2] A. Nakayama, Y. Terashi, H. Uchimura, A. Fukuura, "Conductivity Measurement at the Interface Between the Sintered Conductor and Dielectrics Substrate at Microwave Frequencies", *IEEE Trans. Microwave Theory and Tech.*, vol. 50, no. 7, pp. 1665-1674, July 2002.
- [3] H. Liang, A. Sutono, J. Laskar, W. R. Smith, "Material Parameters Characterisation of Multilayered LTCC and implementation of High Q resonators", *IEEE MTT-S Digest*, pp. 1901-1904, 1999.
- [4] A. E. Fathy, V. A. Pendrick, B. D. Geller, S. M. Perlow, E. S. Tormey, A. Prabhu, S. Tani, "An innovative Semianalytical Technique for ceramic Evaluation at Microwave Frequency", *IEEE Trans. Microwave Theory and Tech*, vol. 50, no. 10, pp. 2247-2252, October 2002.
- [5] S. Vasudevan, A. Shaikh, "Microwave Characterization of Low Temperature Cofired Ceramic System", *Int. Symp. on Advanced Packaging Materials*, pp. 152-157, 1997.
- [6] C. A. Tavernier, R. M. Henderson, J. Papapolymerou, "A Reduced-Size Silicon Micromachined High-Q Resonator at 5.7 GHz", *IEEE Trans. Microwave Theory and Tech*, vol. 50, no. 10, pp. 2305-2314, October 2002.
- [7] H. Hsu, M. J. Hill, J. Papapolymerou, R. W. Ziolkowski, "A Planar X-Band Electromagnetic Band-Gap (EBG) 3 pole filter", *IEEE Microwave and Wireless Components Letters*, vol. 12, No. 7, pp. 255-257, July, 2002.
- [8] R. F. Harrington, *time-Harmonic Electromagnetic Field*, New York: McGraw-Hill, pp. XX, 1961.
- [9] J. P. Raskin, G. Gauthier, L.P. Katehi, G. M. Rebeiz, "W-band Single-Layer Vertical Transition", *IEEE Trans. Microwave Theory and Tech*, vol. 48, no. 1, pp. 161-164, January 2000.
- [10] A. M. Lyons, A. J. Becker, Y. Lee, C. Metz, S. E. Shih, "Connector Interconnections to Transmission Lines For 40 Gb/s Broadband Applications", *IEEE Elec. Comp. and Techn. Conf.*, pp. 1021-1026, 2002.

## ANNEXE

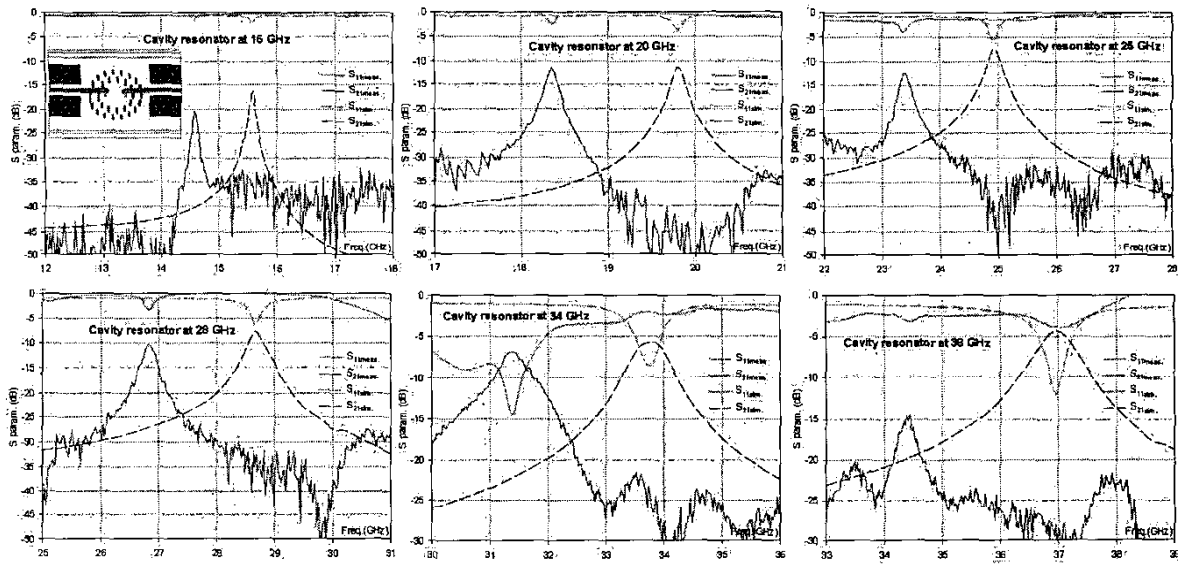


Fig. 5. Simulated vs. measured performance of each cavity resonator.